Threshold Photoelectron−Photoion Coincidence Spectroscopy: Dissociation Dynamics and Thermochemistry of $Ge(CH_3)_4$, $Ge(CH_3)_3Cl$, and $Ge(CH_3)_3Br$

Juan Z. Dávalos,[†,‡] Hideya Koizumi,[†] and Tomas Baer*[,†]

Department of Chemistry, University of North Carolina, Chapel Hill, North Carolina 27599-3290, and Instituto de Química-Física "Rocasolano", CSIC, Serrano 119, 28006, Madrid, Spain

Received: January 13, 2006; In Final Form: March 4, 2006

Threshold photoelectron−photoion coincidence spectroscopy (TPEPICO) has been used to investigate the gas-phase ionic dissociation energies and thermochemistry of Me_4Ge and Me_3GeX, (Me = methyl; X = Cl, Br) molecules. The 0 K dissociation onsets for these species have been measured from the breakdown diagram and the ion time-of-flight distributions, which were modeled with the statistical RRKM theory and DFT calculations. The measured 0 K dissociative photoionization onsets were as follows: $Me_3Ge^+ + Me$ (9.826 ± 0.010 eV); $Me_3Ge^+ + Cl$ (10.796 ± 0.040 eV); $Me_3Ge^+ + Br$ (10.250 ± 0.011 eV); $Me_2GeCl^+ + Me$ (10.402 ± 0.010 eV); and $Me_2GeBr^+ + Me$ (10.333 ± 0.020 eV). These onsets were used to obtain new values for $\Delta_f H^\circ_{298}$ (in kJ/mol) of the neutral molecules Me_3GeCl (−239.8 ± 5.7) and Me_3GeBr (−196.5 ± 4.3), and also for the following ionic species: Me_3Ge^+ (682.3 ± 4.1), Me_2GeCl^+ (621.1 ± 5.8), and Me_2GeBr^+ (657.8 ± 4.7).

1. Introduction

Germanium species such as germane, GeH_4, and its halogenated and alkylated derivatives have been used in the semiconductor industry and chemical vapor deposition (CVD) for years.[1−7] The thermochemistry and bond energies of Ge species is thus of some importance. However, only the heats of formation of a few of these molecules (e.g., GeF_4, $GeCl_2$) are known accurately, while the rest are not well-established or have never been measured. This is the case for tetramethyl germanium and the halogen trimethyl germanium molecules.

The experimental $\Delta_f H^\circ_{298}$ (Me_4Ge) values in the literature range from −87.9 to −134 kJ/mol. Shaulov et al.[8] and Long and Pulford[9] derived values of −87.9 and −102.6 ± 8.3 kJ/mol, respectively, using a static bomb calorimetry method.[10] Steele[11] suggested a value −123 kJ/mol from comparative results of bond-dissociation enthalpies for group IV tetramethyl and tetraphenyl molecules. Lappert et al.[12] proposed a more negative value (−134 ± 13 kJ/mol) several years ago, based on group additivity methods by taking into account the value for $Ge(C_2H_5)_4$ listed by Cox and Pilcher.[13] Two values listed in the NIST webook[14] are −72.8 ± 8.7 and −107.5 ± 6.4 kJ/mol, which are based on an undisclosed review method. In the case of $\Delta_f H^\circ_{298}$ (Me_3GeX) [X = Cl, Br], the heats of formation were estimated by Baldwin et al.[15] from calorimetric results, and these are discussed in this work.

It is evident that reliable experimental heats of formation for several germanium molecules are not available. In a recently submitted paper,[16] we have computed the heats of formation of GeH_4, GeF_4, and $GeMe_4$ at the CCSD(T)/CBS level of theory using MOLPRO, including relativistic effects, core valence correlation, spin−orbit effect, and zero point energy with anharmonic corrections. Our best estimate for the heats of formation of GeF_4 differ by only 2 kJ/mol from the accurate experimental value of −1192 kJ/mol, which is the adjusted average of three experimental results.[16] On the basis of this good agreement, we claim that the same method yields a $\Delta_f H^\circ_{298}$ (Me_4Ge) value of −123 ± 4 kJ/mol with an error that is comparably small. This theoretical value will be used as a basis in this paper to establish the heats of formation of other species, such as the halogenated methyl germanes, for which calculations at a comparable level of theory are beyond current resources.

In this work, we report on the dissociative photoionization and the thermochemical properties, in the gas phase, of neutral and ionic species of alkyl- and halogen-substituted alkyl germanium by the technique of threshold photoelectron photoion coincidence (TPEPICO) spectroscopy. By measuring the 0 K dissociation onset, E_0, based on reaction 1 and using the value in the thermochemical cycle described by eq 2

$$AB + h\nu \rightarrow A^+ + B + e^- \quad (1)$$

$$E_0 = \Delta_f H^\circ_{0K}(A^+) + \Delta_f H^\circ_{0K}(B) - \Delta_f H^\circ_{0K}(AB) \quad (2)$$

it is possible to determine the heat of formation at 0 K of one particular molecule or ion by knowing the value of another two. The conversion of the heat of formation from 0 to 298 K and vice versa can be made by means of the usual thermochemical cycle, given by eq 3

$$\Delta_f H^\circ_{0K} = \Delta_f H^\circ_{298K} - (H^\circ_{298K} - H^\circ_{0K})_{molecule/ion} + \sum(H^\circ_{298K} - H^\circ_{0K})_{elements} \quad (3)$$

where the vibrational frequencies needed to determine the value of $H^\circ_{298K} - H^\circ_{0K}$ for the molecule or ion can be determined from quantum chemical calculations, and those for the elements, in their standard states, are taken from the literature.[17,18] These same sources also provide the $\Delta_f H^\circ_{0K}$ of the atomic elements.

2. Experimental Section

A. Threshold Photoelectron-Photoion Coincidence (TPEPICO) spectrometer. The measurements were performed with

[†] University of North Carolina.
[‡] CSIC.

10.1021/jp060264t CCC: $33.50
Published on Web 03/30/2006

a TPEPICO apparatus which has been described in detail previously.[19] Briefly, the room-temperature sample vapor was ionized with vacuum ultraviolet (VUV) light from an H_2 discharge lamp dispersed by a 1 m normal incidence vacuum monochromator. The VUV wavelengths were calibrated against the hydrogen Lymann-α line. The ions and the electrons were extracted in opposite directions with an electric field of 20 V/cm.

The electrons are velocity-focused [20,21] and detected by two Burle channeltrons, one of them located along the extraction axis and the other located alongside the first one, but separated from it by about 5 mm. Threshold electrons and some energetic (hot) electrons with their velocity directly along the extraction axis are detected by the first channeltron, whereas only hot electrons, with a few millielectronvolts perpendicular to the extraction axis, are detected by the second channeltron. By adopting a hot electron subtraction procedure described previously,[19] we can obtain TPEPICO data with no contamination from "hot" electrons.

The ions are accelerated to 100 eV in the first 5-cm-long accelerated region and to 260 eV before entering a 30-cm-long drift region. The ions are then decelerated to 180 V before entering a 5-cm-long final drift region. The purpose of the final deceleration is to separate fragment ions born in the first drift region from undissociated parent ions. All ions are detected by tandem Burle multichannel plate (MCP) detector at the end of the second drift region.

The electron and ion signals are used as start and stop pulses, respectively, for measuring the ion time-of-flight (TOF), and the TOF for each coincidence event is stored on a multichannel pulse height analyzer. These TPEPICO TOF spectra were used to obtain the fractional abundances of the parent and daughter ions as a function of the photon energy (breakdown diagram) as well as for measuring the ion dissociation rate constants if the dissociation rates are in the microsecond time range. These rates can be extracted from the asymmetric TOF distributions of the daughter ions signal. Separate TPEPICO-TOF distributions were collected for the central and off-axis electron channeltrons.

B. Materials. Tetramethylgermanium (Me_4Ge, purity 98%), trimethylgermanium chloride (Me_3GeCl, purity 98%), and trimethylgermanium bromide (Me_3GeBr, purity 97%) were purchased from Sigma-Aldrich and used without further purification.

3. Quantum Chemical Calculations and Simulation of Experimental Results

Some of the quantum chemical calculations were carried out using the *Gaussian 03* package.[22] The ground-state geometries of the neutral and ionic species were optimized by using density functional theory (DFT), with Becke 3-parameter and Lee−Yang−Parr (B3LYP) functional[23−25] and the 6-311G* basis set. The calculated vibrational frequencies were accepted as is without scaling. An approximate set of transition-state (TS) vibrational frequencies was obtained by stretching the appropriate bond to approximately 4 Å at the B3LYP level of theory. The calculated vibrational frequencies were used to model the data in several ways. The frequencies of the neutral molecules were used to obtain the room-temperature internal energy distribution of our sample, whereas the ion frequencies were required to calculate the ion density of internal energy levels for the rate analysis. Finally, the TS frequencies were required for calculating the sum of states. However, these frequencies were adjusted to fit the rate data.

The 0 K dissociation onset ($Me_3Ge^+ + Me$) was calculated using coupled cluster level of theory at complete basis set (CBS) limit to compare with the experimental dissociative photoionization of Me_4Ge. The detailed description of the theoretical method is described elsewhere.[16] Briefly, the CBS limit is obtained by separate extrapolation of self-consistent field (SCF) and correlation energies using a family of correlation consistent basis sets at the optimized geometry at B3LYP/aug-cc-pVTZ level. Core valence correlation, relativistic effects, and zero point energy including anharmonic corrections are taken into account. The core valence correlation and relativistic effects are calculated including 3s3p3d orbitals of germanium as in the previous study.[16] The symmetries of $GeMe_4$ (tetrahedral) and $GeMe_3^+$ (planar) were assumed. All coupled cluster calculations were performed using the MOLPRO quantum chemistry package.[26]

It was possible at this level of theory to calculate the dissociation onset for methyl loss from $GeMe_4$. However, similar calculations for the trimethyl halo germanium reactions, which involve two heavy atoms, were beyond our capability.

Because all molecules studied here include three or four methyl internal rotors, some of the vibrational frequencies used in the 298 K conversion using eq 3 are corrected for hindered rotor effects at the B3LYP/aug-cc-pVTZ level of theory. These effects are sometimes important when the vibrational frequencies corresponding to internal rotations are less than 100 cm^{-1}. We calculated these explicitly for the Me_4Ge and approximated the rotor effect for the Me_3GeX compounds using the Me_4Ge calculation as a guide. The effects (less than 0.5 kJ/mol) were found to be minor.

If the dissociation reaction is rapid ($k > 10^7$ s^{-1}) the TPEPICO TOF peak shapes are symmetric, and only their total areas are interesting. In this case, one can obtain directly the corresponding breakdown diagram, which is the fractional abundance of parent and daughter ions. Breakdown diagrams corresponding to processes with a single product ion are modeled in terms only of the neutral thermal energy distribution[27] in which it is assumed that any parent ion with internal energy (photon energy plus molecule thermal energy) in excess of the dissociation energy, E_0, will dissociate immediately. It is thus possible to extract a precise 0 K dissociation onset (E_0), which is defined as the photon energy at which all parent ion signal disappears. If the fast reaction includes competitive or parallel dissociation steps, the first reaction channel is analyzed as just mentioned. However, the calculation of the second onset is more difficult and requires some assumptions about the TSs for the two competing reactions. According to the statistical theory of unimolecular decay (RRKM),[28,29] the ratio of the rates for the two competitive reactions above the second onset is given as the ratio of the sum of states in the transition state

$$\frac{k_1}{k_2} = \frac{\sigma_1 N_1^{\#}(E - E_{01})}{\sigma_2 N_2^{\#}(E - E_{02})} \quad \text{for } E > E_{02} \tag{4a}$$

where E_{0i} are the activation energies for the first and second channels, $N_i^{\#}(E - E_{0i})$ are the sums of states of the transition state from 0 to $E - E_{0i}$ for the two channels, and σ_i are the symmetry parameters for the two reaction channels.

If the dissociation reaction is slow ($k < 10^7$ s^{-1}), which is the case if the ion has a large number of vibrations and the activation energy is large, the daughter ion TOF peak shapes are asymmetric, because the parent ions (metastable ions) dissociate slowly in the first acceleration region. The rate constant for unimolecular decay is given by the RRKM theory as

$$k = \frac{\sigma N^{\#}(E - E_0)}{h\rho(E)} \quad (4b)$$

where $\rho(E)$ is the density of states of the molecule (or ion) at energy E. This analysis is more complicated than the case of fast reactions, because it presents additional problems and constraints. For instance, the subtraction procedure in the TOF spectra to correct the contribution of "hot" electrons is done channel by channel (not just the peak areas, but the spectra themselves) as described previously.[30] The TOF distributions and breakdown diagrams are simulated using rate constants calculated by RRKM statistical theory along with the thermal energy distribution.

The simulations were carried out using the following information: the vibrational frequencies of the neutral molecule which yield the sample's room-temperature internal energy distribution, the ion and transition state frequencies of the sample, the ionization energy, and the acceleration electric fields and drift distances of the ion time-of-flight system. The dissociation energies and the lowest three or four TS vibrational frequencies were adjusted to fit the simulated to the experimental data. The variable parameters were optimized using a downhill simplex method.[31,32]

The uncertainties for the dissociation onsets were obtained following the procedure described in previous studies,[33,34] which involves checking the flexibility of the fit upon variations in the adjustable parameters. The error limits in E_0 were then established by noting its value when the fit to the data became significantly worse.

4. Results and Discussion

A. Dissociation of Me_4Ge. Thermochemistry of Trimethyl Germanium Ion (Me_3Ge^+). The dissociation process for this molecule is rapid, and the 0 K dissociation onset (E_0) was obtained from fitting the breakdown diagram (Figure 1) by varying only the E_0 value. Reaction 5 shows the only dissociation path for ionized Me_4Ge in the range 9.60−10.28 eV. The

$$Me_4Ge + h\nu \rightarrow Me_3Ge^+ + Me^{\bullet} + e^- \quad (5)$$

derived 0 K onset for methyl loss is $E_0 = 9.826 \pm 0.010$ eV. Using eq 2 with the heats of formation shown in Table 1, we can obtain the heat of formation at 0 K of the trimethyl germanium ion, $\Delta_f H^\circ_{0K}$ (Me_3Ge^+) = 705.8 ± 4.1 kJ/mol, which is converted to $\Delta_f H^\circ_{298}$ (Me_3Ge^+) = 682.3 ± 4.1 kJ/mol. The only literature value for this dissociative ionization onset was reported by Lappert et al.[12] in 1971 who obtained 10.05 ± 0.14 eV by electron ionization, which is some 0.22 eV above our value. Nevertheless, their onset energy, when combined with an estimated heat of formation of the Me_4Ge of −134 kJ/mol, yielded a Me_3Ge^+ heat of formation that is only 8 kJ/mol higher than ours, clearly the result of two errors that cancel. The other Me_3Ge^+ energy was one obtained by a MINDO calculation of Dewar et al.[35] who reported a value that is only 1.6 kJ/mol lower than ours, which, given the crude approximations inherent in the MINDO approach, must also arise from the cancellation of several errors.

The geometry of the Me_3Ge^+ ion has C_{3h} symmetry at B3LYP/aug-cc-pVTZ level of theory. The Ge−C bond length, 1.928 Å, is much shorter than that of Me_4Ge, 1.975 Å, because of smaller repulsive interactions between methyl groups. Our CCSD(T)/CBS theoretical onset of reaction 5 of 9.86 eV is in excellent agreement with our experimental result. Although the discrepancy of 3 kJ/mol is well within our theoretical uncertainties, it is worthwhile to check the self-consistency of our approach. The 0 K heat of formation of Me_3Ge^+ obtained using the theoretical onset of this reaction is 709 kJ/mol. The corresponding value based on the total atomization energy using the same level of theory[16] is 711 kJ/mol. The discrepancy of 2 kJ/mol is a result of the indirect relativistic and core valence correlation corrections, which are exactly 2 kJ/mol, and which were used to obtain an accurate heat of formation of Me_4Ge.[16] The correction requires the knowledge of an accurate molecular geometrical parameter of Me_3Ge^+ ion from either highly accurate experiment or high-level theory including relativistic and core valance correlation. Obviously, such information is not available for the Me_3Ge^+ ion. Assuming the indirect correction is identical to that of Me_4Ge, we obtain 709 kJ/mol, which now agrees perfectly. It is worthwhile to note that the methyl radical heat of formation obtained at the same level of theory differs by less than 1 kJ/mol from the experimental value.

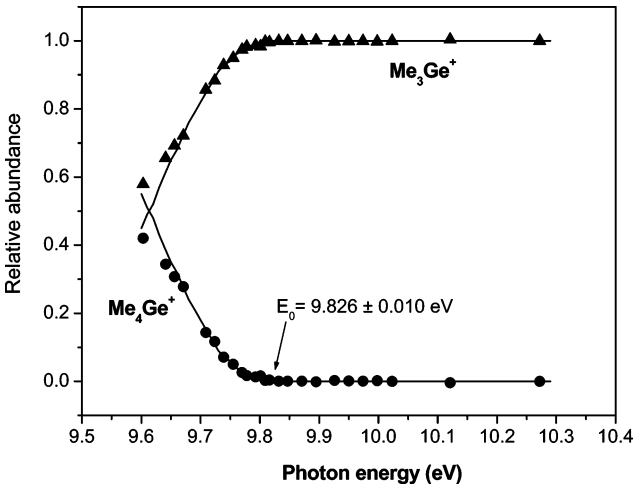

Figure 1. The breakdown diagram for Me_4Ge^+ in the 9.60−10.28 eV range. The solid line through the experimental points is obtained by modeling a fast dissociation with a room-temperature thermal energy distribution. The indicated onset is derived from the fit.

B. Dissociation of Me_3GeCl. Thermochemistry of Neutral Molecule Me_3GeCl and Ionic Fragment Me_2GeCl^+. The symmetric daughter ion TOF distributions indicate that the dissociation of Me_3GeCl^+ is rapid. Reactions 6 show the parallel dissociation steps of this ion in the range from 9.95 to 11.83 eV. The first derived 0 K dissociation onset is $E_{01} = 10.402 \pm 0.010$ eV, which corresponds to the methyl loss reaction. The

$$Me_3GeCl + h\nu \rightarrow \begin{cases} Me_2GeCl^+ + Me^{\bullet} + e^- & E_{01} \\ Me_3Ge^+ + Cl^{\bullet} + e^- & E_{02} \end{cases} \quad (6)$$

fit of its onset is determined, as for Me_4Ge case, only by assuming the calculated neutral thermal energy distribution and varying the 0 K dissociation energy. The second dissociation onset (E_{02}) at a somewhat higher photon energy is observed in competition with first dissociation. As is evident in Figure 2, this onset is much less sharp than first one. This is because of the competitive shift of the second onset relative to the first, which shifts its onset to higher energy.[38−40] To fit the breakdown diagram in Figure 2, the transition state (TS) frequencies of the two reaction channels are required. Because the rate constants are larger than experimentally measurable by our TPEPICO experiment, only the relative rate constants are important. Thus, the TS frequencies for the methyl loss reaction were taken directly from the DFT calculations, while the four lowest-

TABLE 1: Auxiliary and Derived Thermochemical Data (in kJ/mol)

	$\Delta_f H^\circ_{0K}$ [a]	$(H^\circ_{298K} - H^\circ_{0K})$ [b]	$\Delta_f H^\circ_{298K}$ [a]	$\Delta_f H^\circ_{298K}$ (lit. values)
Me_4Ge	-92 ± 4 [c]	28.9	-123 ± 4 [c]	-87.9,[d] -102.6 ± 8.3,[e] -72.8 ± 8.7,[f] -107.5 ± 6.4,[f] -123,[g] -134 ± 13[h]
Me_3GeCl	-216.3 ± 5.7	26.9	-239.8 ± 5.7	-266.1 ± 8.8[i]
Me_3GeBr	-165.3 ± 4.3	26.9	-196.5 ± 4.3	-222.2 ± 8.8[i]
Me_3Ge^+	705.8 ± 4.1	22.4	682.3 ± 4.1	680.7,[j] 690.3,[h] 685.5[k]
Me_2GeCl^+	637.1 ± 5.8	20.8	621.1 ± 5.8	
Me_2GeBr^+	681.4 ± 4.7	20.8	657.8 ± 4.7	
Me	150.3 ± 0.4[l]			

[a] Determined from current TPEPICO dissociation onsets, unless otherwise stated. [b] Obtained using vibrational frequencies calculated at the B3LYP/aug-cc-pVTZ level with hindered rotor corrections. [c] Calculated and reported by Koizumi et al.[16] [d] Shaulov et al.[8] [e] Long et al. [9] [f] NIST webside.[14] [g] Steele.[11] [h] Lappert et al.[12] [i] Baldwin et al.[15] [j] Dewar et al.[35] [k] Calculated at the CCSD(T)/CBS level of theory. [l] From Weitzel et al.[36] and Blush et al.[37]

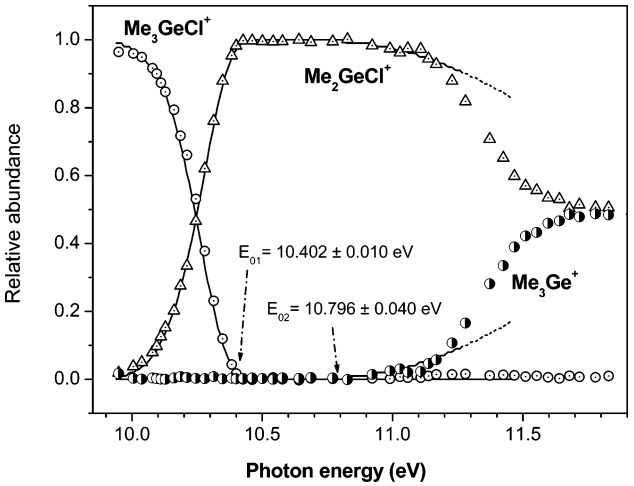

Figure 2. The breakdown diagram for Me_3GeCl^+ in the 9.95−11.83 eV range, showing the two parallel dissociation steps, loss Me and loss Cl. Solid lines are simulated by taking into account the thermal energy distribution as well as rate constants.

frequency modes for the second dissociation channel were varied until a best fit was obtained. The errors associated with the higher-energy onsets are greater, because the data are fitted by varying two parameters, E_0 and the transition-state frequencies.[41]

It is evident in Figure 2 that the breakdown diagram at energies higher than 11.20 eV does not follow the simulation. In fact, it is impossible to fit the breakdown diagram above 11.3 eV, which suggests that the reaction is not statistical at these energies. There are two experimental pieces of evidence that support this claim. First of all, we note that, at an energy of 11.7 eV, the TOF peak width of the Cl loss peak is significantly broader (14 channels wide) than the TOF peak width of the methyl loss fragment (10 channels wide), even though the excess energy for the methyl loss peak is greater. The fragment ion peak width scales with the square of its translational energy. The peak width analysis indicates that the methyl loss peak width is consistent with statistical partitioning of the energy into translations, whereas the broad Cl loss peak indicates that more than twice as much of the excess energy is channeled into translational energy, than is predicted by the statistical theory. The second piece of evidence that suggests nonstatistical dissociation lies in the photoelectron spectrum of $GeMe_3Cl$[42] shows that we have a Franck−Condon gap at 11 eV and a new photoelectron spectroscopy (PES) peak that rises at about 11.3 eV. If this excited electronic state is repulsive and dissociates exclusively by Cl loss, then the reaction will not be statistical, and we lose our ability to analyze the shape of the breakdown diagram. Such dissociative states are not uncommon for the case of halogenated ions.[43−46] A particularly relevant example is t-C_4H_9I, in which the ground ionic state dissociates statistically and the excited ionic state does not.[47] For this reason, we modeled only the very initial parts of the Me_3Ge^+ peak in Figure 2. With the above assumptions, the derived onset for the chlorine loss dissociation channel, at 0 K, is $E_{02} = 10.796 \pm 0.040$ eV. Its error is considerably larger because of the nonstatistical nature of the reaction at higher energies. From this onset and the heats of formation of chlorine atom and of Me_3Ge^+ ion (determined before), we obtain the 0 K heat of formation of -216.3 ± 5.7 kJ/mol for the neutral molecule, Me_3GeCl, which is converted to $\Delta_f H^\circ_{298}$ (Me_3GeCl) $= -239.8 \pm 5.7$ kJ/mol at 298 K. As one can see in Table 1, this value is almost 26 kJ/mol more positive than that estimated by Baldwin et al.[15] With this Me_3GeCl heat of formation, we can use the first onset, E_{01}, and the heat of formation of the methyl radical, to obtain a heat of formation of 637.1 ± 5.8 kJ/mol for Me_2GeCl^+ ion at 0 K, which is converted to $\Delta_f H^\circ_{298}$ (Me_2GeCl^+) $= 621.1 \pm 5.8$ kJ/mol at 298 K.

C. Dissociation of Me_3GeBr. Thermochemistry of Neutral Molecule Me_3GeBr and Ionic Fragment Me_2GeBr^+. The dissociation of Me_3GeBr (reaction 7) also proceeds via halogen and methyl loss steps. But, in this case, the bromine loss occurs at a lower energy than the methyl loss reaction. Because of the greater bond energy, this reaction is sufficiently slow at the dissociation limit to exhibit asymmetric TOF distributions. The

$$Me_3GeBr + h\nu \rightarrow \begin{cases} Me_3Ge^+ + Br^\bullet + e^- & E_{01} \\ Me_2GeBr^+ + Me^\bullet + e^- & E_{02} \end{cases} \quad (7)$$

TOF mass spectra were acquired in the photon energy range 9.86−10.55 eV, examples of which are shown in Figure 3. Figure 4 shows one of these time-of-flight distributions, in which the various peaks are evident. The cluster of parent ion peaks (Me_3GeBr^+, m/z 198) at 32 μs shows the partially resolved isotopic distribution resulting from the many Ge isotopes and the two Br isotopes. The two slightly asymmetric peaks correspond to daughter ions formed by loss of Br and loss of Me: Me_3Ge^+ (m/z 119, 24.8 μs) and Me_2GeBr^+ (m/z 183, 30.8 μs), respectively. They are asymmetric because the product ions are generated as the parent ions are accelerating in the first extraction region. Finally, a fourth small broad peak ("drift" peak) around 32.9 μs is associated with parent ions that dissociate in the 30-cm-long drift region. The fractional abundances of the parent and daughter ions are shown in the breakdown diagram in Figure 5. The "drift" peak was included in the parent ion signal, so that only those ions that dissociated in the first acceleration region are considered fragment ions. The TOF distributions and the breakdown diagram have been modeled by varying the dissociation onsets of the Me loss and

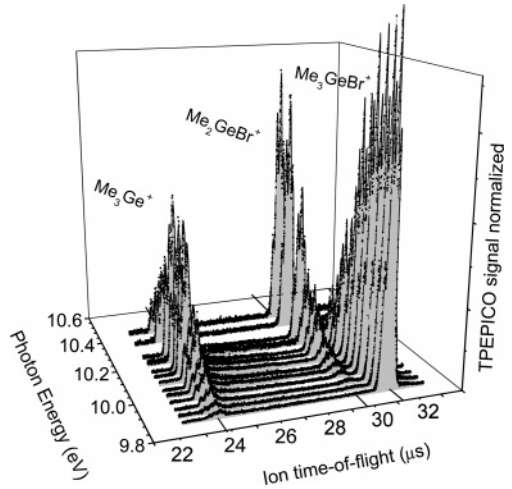

Figure 3. TPEPICO ion time-of-flight distributions for Me_3GeBr at several selected photon energies in the range 9.86−10.43 eV. Points are the experimental data, while solid lines limited by shadow areas show the simulated TOF distributions.

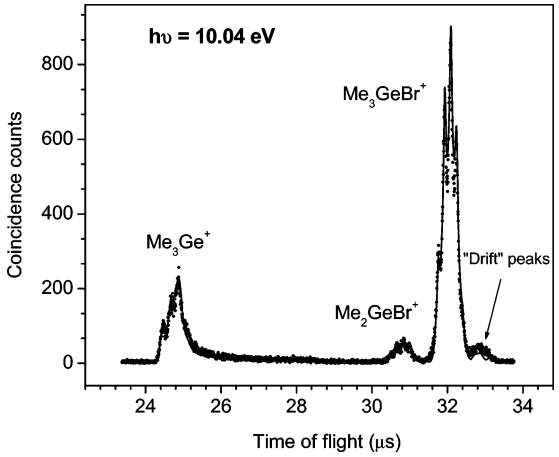

Figure 4. Typical time-of-flight distribution of the Me_3GeBr^+ ions at 10.04 eV photon energy, showing the fit of the model to the slightly asymmetric peak for the loss Br. The "drift" peak is a result of parent ions that dissociate in the drift region. It appears after the parent ion because the ions were slowed before entering the final drift region. Solid line is simulated as described in text.

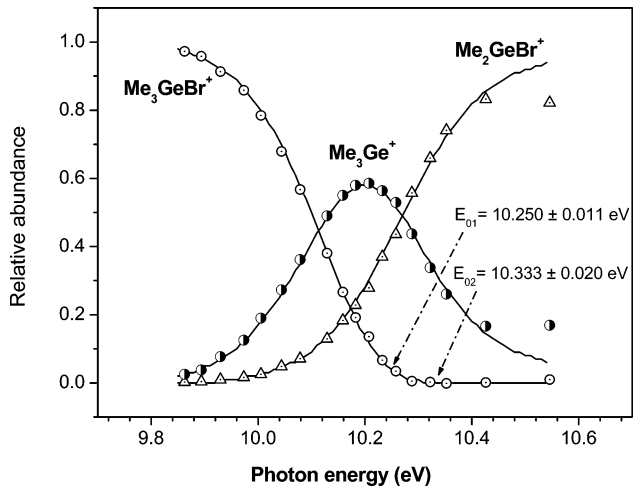

Figure 5. The breakdown diagram for Me_3GeBr^+ ions in the 9.86−10.55 eV range. Solid lines are simulated as described in text.

Br loss reactions as well as the TS vibrational frequencies. The solid lines in Figures 3−5 are the best fits obtained by varying

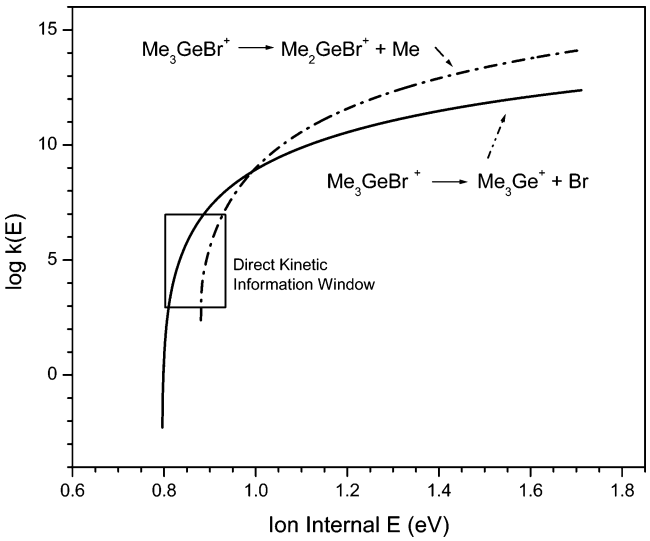

Figure 6. The RRKM rate constants that fit both the TOF distributions and the breakdown diagram for trimethyl germanium bromide.

the two 0 K dissociation onsets and the two sets of transition-state frequencies.

The rate constants shown in Figure 6 are the optimum $k(E)$ functions which have been determined from the simulation of the TOF distribution and breakdown diagram. In the lower part of the energy range (<10.34 eV), both dissociation rates are slow ($k < 10^7$ s^{-1}) so that the parent ions dissociate during their whole trajectory. This explains the slightly asymmetric peaks particularly for the fragment Me_3Ge^+ in the 24.28−26.30 μs range. The activation entropies of the two dissociation channels calculated at 600 K were 59.4 and 20.7 $J\cdot mol^{-1}\cdot K^{-1}$ for loss bromide and loss methyl, respectively. Both are positive, which indicates that these reactions proceed via loose transition states. As one also can see in Figure 6, the Br loss reaction rate increases more slowly than the methyl loss rate. The derived dissociation onsets at 0 K are $E_{01} = 10.250 \pm 0.011$ eV (loss Br) and $E_{02} = 10.333 \pm 0.020$ eV (loss Me). The error here is smaller than that quoted for the Cl loss reaction in $GeMe_3Cl^+$, because this reaction seems to be statistical over the whole energy range investigated, and we can use the measured rate constants to help establish the 0 K onset.

The E_{01} value for the Br loss reaction combined with the heats of formation of the Br atom [18] and of Me_3Ge^+ (obtained in this work) leads to a 0 K heat of formation of -165.3 ± 4.3 kJ/mol for the neutral molecule Me_3GeBr, which converts to $\Delta_f H^\circ_{298}$ (Me_3GeBr) = -196.5 ± 4.3 kJ/mol at 298 K. This heat of formation combined with E_{02} for Me loss leads to the 0 K heat of formation of 681.4 ± 4.7 kJ/mol for the dimethylgermanium bromide ion, which converts at 298 K to $\Delta_f H^\circ_{298}$ (Me_2GeBr^+) = 657.8 ± 4.7 kJ/mol.

Some years ago, Baldwin et al.[15] determined the heats of formation of neutral halogen trimethyl germanium, Me_3GeX (X = Cl, Br), by measuring the enthalpy associated with the hydrolysis process described by eq 8. Their measurements of

$$Me_3GeX + (1/2)H_2O \rightarrow (1/2)(M_3Ge)_2O + HX[55H_2O] \quad \Delta_r H \quad (8)$$

$\Delta_r H$ for X = Cl and Br were −7.1 and −2.1 kJ/mol, respectively. Inasmuch as the heat of formation of $(Me_3Ge)_2O$ was (and still is) unavailable, it was estimated from the heat of formation of $(Et_3Ge)_2O$ and adjusted for the ethyl/methyl group substitutions. This led to liquid-phase heats of formation, which

they converted to gas-phase values by estimating the vapor pressure using Trouton's rule. They thus reported the gas-phase heats of formation of −266.1 and −222.2 kJ/mol for Me_3GeCl and Me_3GeBr, respectively. Although these values differ from ours by nearly 26 kJ/mol, it is perhaps significant that the difference between these heats of formation ($\Delta(\Delta_f H^\circ_{298}) = 43.9$ kJ/mol) does not depend on the doubtful value of $\Delta_f H^\circ_{298}$ ($(Me_3Ge)_2O$). In fact, the Baldwin heat of formation difference is practically the same as our value of 43.3 kJ/mol reported here. The disagreement in the Baldwin and current measurements can thus be attributed primarily to their estimated heat of formation of $(Me_3Ge)_2O$.

Conclusions

Threshold photoelectron and photon coincidence (TPEPICO) technique have been used to study the dissociative photoionization and thermochemistry of a set of germanium compounds: Me_4Ge, Me_3GeCl, and Me_3GeBr. From the analysis of the breakdown diagrams and the simulation of time-of-flight spectra (particularly for Me_3GeBr case), we have obtained accurate dissociation onsets, which were used to find an accurate $\Delta_f H^\circ_{298}$ (Me_3Ge^+) of 682.3 ± 4.1 kJ/mol. This value has been used to obtain the $\Delta_f H^\circ_{298}$ of −239.8 ± 5.7 and −196.5 ± 4.3 kJ/mol for the neutral molecules Me_3GeCl and Me_3GeBr, respectively, which in turn were used to determine the heats of formation (not reported in the literature) of 621.1 ± 5.8 and 657.8 ± 4.7 kJ/mol for the ionic fragments Me_2ClGe^+ and Me_2BrGe^+, respectively.

Acknowledgment. The authors thank the U.S. Department of Energy for support of this work. J.Z. Dávalos acknowledges the Ministerio de Educación, Cultura y Deporte of Spain for the PR2004-0031 Grant. We are also grateful to Prof. Balint Sztaray for continued updating of the program used to analyze the TOF distributions and the breakdown diagrams.

References and Notes

(1) Bogumilowicz, Y.; Hartmann, J. M.; Truche, R.; Campidelli, Y.; Rolland, G.; Billon, T. *Semicond. Sci. Technol.* **2005**, *20*, 127.

(2) Hartmann, J. M.; Damlencourt, J.-F.; Bogumilowicz, Y.; Holliger, P.; Rolland, G.; Billon, T. *J. Cryst. Growth* **2005**, *274*, 90.

(3) Rapiejko, C.; Gazicki-Lipman, M.; Klimek, L.; Szymanowski, H.; Strojek, M. *Thin Solid Films* **2004**, *469*−*470*, 173.

(4) Szmidt, J.; Gazicki-Lipman, M.; Szymanowski, H.; Mazurczyk, R.; Werbowy, A.; Kudla, A. *Thin Solid Films* **2003**, *441*, 192.

(5) Li, Q.; Li, G.; Xu, W.; Xie, Y.; Shaefer, H. F. *J. Chem. Phys.* **1999**, *111*, 7945.

(6) Waltenburg, H. N.; Yates, J. T., Jr. *Chem. Rev.* **1995**, *95*, 1589.

(7) Ho, P.; Melius, C. F. *J. Phys. Chem.* **1990**, *94*, 5120.

(8) Shaulov, Y. K.; Fedorov, A. K.; Genchel, V. G. *Russ. J. Phys. Chem. (Engl. Trans.)* **1969**, *43*, 744.

(9) Long, L. H.; Pulford, C. I. *J. Chem. Soc., Faraday Trans.* **1986**, 567.

(10) Pilcher, G. *Energetics of Organometallic Species, Series C: Mathematical and Physics Science*; Martinho Simoes, J. A., Ed.; Kluger Academic Publishers: Boston, 1992; Vol. 367, p 9.

(11) Steele, W. V. *J. Chem. Thermodyn.* **1983**, *15*, 595−601.

(12) Lappert, M. F.; Pedley, J. B.; Simpson, J.; Spalding, T. R. *J. Organomet. Chem.* **1971**, *29*, 195.

(13) Cox, J. D.; Pilcher, G. *Thermochemistry of organic and organometallic compounds*; Academic Press: London, 1970.

(14) http://webbook.nist.gov/chemistry; 2005.

(15) Baldwin, J. C.; Lappert, M. F.; Pedley, J. B.; Poland, J. S. *J. Chem. Soc., Dalton Trans.* **1972**, 1943.

(16) Koizumi, H.; Dávalos, J. Z.; Baer, T. *Chem. Phys.* **2005**, http://dx.doi.org/10.1016/j.chemphys.2005.11.002.

(17) Wagman, D. D.; Evans, W. H. E.; Parker, V. B.; Schum, R. H.; Halow, I.; Mailey, S. M.; Churney, K. L.; Nuttall, R. L. The NBS Tables of Chemical Thermodynamic Properties. *J. Phys. Chem. Ref. Data* **1982**, *11*, Suppl. 2.

(18) Chase, M. W., Jr. *NIST-JANAF Thermochemical Tables*, 4th ed.; Journal of Physical and Chemical Reference Data Monograph 9; American Institute of Physics: New York, 1998; pp 1−1951.

(19) Sztáray, B.; Baer, T. *Rev. Sci. Instrum.* **2003**, *74*, 3763.

(20) Chandler, D. W.; Parker, D. H. *Adv. Photochem.* **1999**, *25*, 59.

(21) Suits, A. G., Continetti, R. E., Eds *Imaging in Chemical Dynamics*; ACS Symposium Series 770; American Chemical Society: Washington, DC, 2001.

(22) Frisch, M. J.; Trucks, G. W.; Schlegel, H. B.; Scuseria, G. E.; Robb, M. A.; Cheeseman, J. R.; Montgomery, J. A., Jr.; Vreven, T.; Kudin, K. N.; Burant, J. C.; Millam, J. M.; Iyengar, S. S.; Tomasi, J.; Barone, V.; Mennucci, B.; Cossi, M.; Scalmani, G.; Rega, N.; Petersson, G. A.; Nakatsuji, H.; Hada, M.; Ehara, M.; Toyota, K.; Fukuda, R.; Hasegawa, J.; Ishida, M.; Nakajima, T.; Honda, Y.; Kitao, O.; Nakai, H.; Klene, M.; Li, X.; Knox, J. E.; Hratchian, H. P.; Cross, J. B.; Bakken, V.; Adamo, C.; Jaramillo, J.; Gomperts, R.; Stratmann, R. E.; Yazyev, O.; Austin, A. J.; Cammi, R.; Pomelli, C.; Ochterski, J. W.; Ayala, P. Y.; Morokuma, K.; Voth, G. A.; Salvador, P.; Dannenberg, J. J.; Zakrzewski, V. G.; Dapprich, S.; Daniels, A. D.; Strain, M. C.; Farkas, O.; Malick, D. K.; Rabuck, A. D.; Raghavachari, K.; Foresman, J. B.; Ortiz, J. V.; Cui, Q.; Baboul, A. G.; Clifford, S.; Cioslowski, J.; Stefanov, B. B.; Liu, G.; Liashenko, A.; Piskorz, P.; Komaromi, I.; Martin, R. L.; Fox, D. J.; Keith, T.; Al-Laham, M. A.; Peng, C. Y.; Nanayakkara, A.; Challacombe, M.; Gill, P. M. W.; Johnson, B.; Chen, W.; Wong, M. W.; Gonzalez, C.; Pople, J. A. *Gaussian 03*, revision A.04; Gaussian, Inc.: Pittsburgh, PA, 2004.

(23) Becke, A. D. *J. Chem. Phys.* **1993**, *98*, 5648.

(24) Lee, C.; Yang, W.; Parr, R. G. *Phys. Rev. B* **1988**, *37*, 785.

(25) Stephens, P. J.; Devlin, F. J.; Chabalowski, C. F.; Frisch, M. J. *J. Phys. Chem.* **1994**, *98*, 11623.

(26) Werner, H.-J.; Knowles, P. J. MOLPRO, a package of ab initio programs, version 2002.6; Amos, R. D., Bernhardsson, A., Berning, A., Celani, P., Cooper, D. L., Deegan, M. J. O., Dobbyn, A. J., Eckert, F., Hampel, C., Hetzer, G., Knowles, P. J., Korona, T., Lindh, R., Lloyd, A. W., McNicholas, S. J., Manby, F. R., Meyer, W., Mura, M. G., Nicklass, A., Palmieri, P., Pitzer, R., Rauhut, G., Schütz, M., Schumann, U., Stoll, H., Stone, A. J., Tarroni, R., Thorsteinsson, T., Werner, H.-J., Eds.; University of Birmingham, Birmingham, UK., 2002; http://www.molpro.net.

(27) Fogleman, E. A.; Koizumi, H.; Kercher, J. P.; Sztáray, B.; Baer, T. *J. Phys. Chem. A* **2004**, *108*, 5288.

(28) Baer, T.; Hase, W. L. *Unimolecular Reaction Dynamics: Theory and Experiments*; Oxford University Press: New York, 1996.

(29) (a) Kassel, L. S. *J. Phys. Chem.* **1928**, *32*, 225. (b) Marcus, R. A.; Rice, O. K. *J. Phys. Colloid Chem.* **1951**, *55*, 894. (c) Rice, O. K.; Ramsperger, H. C. *J. Am. Chem. Soc.* **1927**, *49*, 1617.

(30) Baer, T.; Sztáray, B.; Kercher, J. P.; Lago, A. F.; Bödi, A.; Scull C.; Palathinkal, D. *Phys. Chem. Chem. Phys.* **2005**, *7*, 1507.

(31) Nelder, J. A.; Mead, R. *Comput. J.* **1965**, *7*, 303.

(32) Press, W. H.; Teukolsky, S. A.; Vetterling, W. T.; Flannery, B. P. *Numerical recipes in C. The art of scientific computing*, 2nd ed.; Cambridge University Press: Cambridge, 1992; pp 408−412.

(33) Li, Y.; Sztáray, B.; Baer, T. *J. Am. Chem. Soc.* **2001**, *123*, 9388.

(34) Bodi, A.; Kercher, J. P.; Baer, T.; Sztaray, B. *J. Phys. Chem. B* **2005**, *109*, 8393.

(35) (a) Dewar, M. J. S.; Grady, G. L.; Healy, E. F. *Organometallics* **1987**, *6*, 186.

(36) Dewar, M. J. S.; Thiel, W. *J. Am. Chem. Soc.* **1977**, *99*, 4899.

(37) Weitzel, K. M.; Malow, M.; Jarvis, G. K.; Baer, T.; Song, Y.; Ng, C. Y. *J. Chem. Phys.* **1999**, *111*, 8267.

(38) Blush, J. A.; Chen, P.; Wiedmann, R. T.; White, M. G. *J. Chem. Phys.* **1993**, *98*, 3557−3559.

(39) Chupka, W. A. *J. Phys. Chem.* **1959**, *30*, 191.

(40) Lifshitz, C. *Mass Spectrom. Rev.* **1982**, *1*, 309.

(41) Huang, F. S.; Dunbar, R. C. *J. Am. Chem. Soc.* **1990**, *112*, 8167.

(42) Lago, A. F.; Kercher, J. P.; Bodi, A.; Sztaray, B.; Miller, B.; Wurzelmann, D.; Baer, T. *J. Phys. Chem. A* **2005**, *109*, 1802.

(43) Flamini, A.; Semprini, E.; Stefani, F. *J. Chem. Soc., Dalton Trans.* **1976**, 731.

(44) Low, K. G.; Hampton, P. D.; Powis, I. *Chem. Phys.* **1985**, *100*, 401.

(45) Powis, I. *Mol. Phys.* **1980**, *39*, 311.

(46) Simm, I. G.; Danby, C. J.; Eland, J. H. D. *Int. J. Mass Spectrom. Ion Processes* **1974**, *14*, 285.

(47) Miller, B. E.; Baer, T. *Chem. Phys.* **1985**, *85*, 39.

(48) Oliveira, M. C.; Baer, T.; Olesik, S.; Almoster Ferreira, M. A. *Int. J. Mass Spectrom. Ion Processes* **1988**, *82*, 299.